Available online at www.sciencedirect.com

SciVerse ScienceDirect

Ceramics International 39 (2013) 7951–7957

CERAMICS INTERNATIONAL

www.elsevier.com/locate/ceramint

Influence of the heat treatment on mechanical properties and oxidation resistance of SiC–Si_3N_4 composites

A. Kovalčíková[a,*], J. Dusza[a], P. Šajgalík[b]

[a]Institute of Materials Research, Slovak Academy of Sciences, Watsonova 47, 040 01 Košice, Slovak Republic
[b]Institute of Inorganic Chemistry, Slovak Academy of Sciences, Dúbravská cesta 9, 845 36 Bratislava 45, Slovak Republic

Received 11 February 2013; accepted 15 March 2013
Available online 2 April 2013

Abstract

The basic mechanical properties and oxidation behaviour of liquid-phase-sintered SiC–Si_3N_4 composites were investigated as a function of the heat treatment at oxidising condition at 1350 °C/0–204 h. The results were compared to those obtained for a reference silicon carbide material, prepared by the same fabrication route. The heat treatment at higher temperature had a positive effect on fracture toughness values but no changes of hardness were observed. It was shown that the oxidation resistance increases with increasing temperature of heat treatment from 1650 °C to 1850 °C. Oxidation always followed parabolic rate law indicating diffusion as the rate limiting mechanisms. The addition of silicon nitride content had no significant influence on oxidation resistance of SiC–Si_3N_4 composites.

Keywords: C. Mechanical properties; Heat treatment; SiC–Si_3N_4 composites; Oxidation resistance

1. Introduction

Silicon carbide and silicon nitride have been recognised as important structural ceramics because of their good combination of mechanical and thermal properties. SiC ceramics show good wear, oxidation and creep resistance at high temperatures, but relatively low fracture toughness. On the contrary, Si_3N_4 ceramics exhibit higher fracture toughness and good flexural strength, but lower resistance to oxidation at high temperatures [1]. The ceramic components to be properly applied in high temperature need to have a high resistance to thermal shock and oxidation, thermal fatigue, corrosion, and resistance to creep deformation.

The room and high temperature properties of liquid-phase-sintered (LPS) SiC ceramics strongly depend on their microstructure. The microstructure of sintered SiC highly depends on the starting powder. Sintering of α-SiC powder can result in fine-grain equaixed grains. The sintering of β-SiC powders leads to the formation of coarsened, elongated morphology which reflect the β-SiC to α-SiC transformation resulting from the high applied temperatures (1800–2000 °C) [2–4]. Elongated grains have been shown to increase fracture toughness by crack bridging or crack deflection due to weak interface boundaries, but coarsening leads to an increase of the size of the critical flaw which degrades flexural strength [5–10].

There are two effective methods for improving the high-temperature properties of silicon carbide materials to increase the refractoriness of the grain boundary phase and to promote crystallisation of the amorphous phase. This can be achieved by the selection of appropriate additives and chemical compositions [11]. A problem associated with the use of additives is the degradation of high temperature properties due to residual grain boundary phase. Sintering additives such as Al_2O_3–Y_2O_3 and AlN–Y_2O_3 were extensively used to obtain dense LPS-SiC ceramics [12–15]. These oxides react with SiO_2 which is always present at the surface of SiC and AlN particles and form an oxynitride melt. Jensen et al. [16] reported that yttrium aluminium garnet (YAG) in the grain boundary phase of SiC sintered with Al_2O_3 and Y_2O_3 dramatically increase the oxidation rate at 1350 °C due to a possible reaction between SiO_2 and YAG that forms a low viscosity liquid. In order to change the crystalline nature of the grain boundary phase different types of rare-earth oxides such as Yb_2O_3, Er_2O_3, Lu_2O_3, Sc_2O_3 and Sm_2O_3 were later used [17–20]. SiC–AlN–RE_2O_3 systems showed favourable oxidation resistance due to

*Corresponding author. Tel.: +421 55 792 2463; fax: +421 55 792 2408.
E-mail address: akovalcikova@imr.saske.sk (A. Kovalčíková).

0272-8842/$ - see front matter © 2013 Elsevier Ltd and Techna Group S.r.l. All rights reserved.
http://dx.doi.org/10.1016/j.ceramint.2013.03.059

Table 1
Chemical composition and heat treatment regimes of the investigated materials.

Samples	Heat treatment	Composition [wt%]			
		SiC	Si_3N_4	Y_2O_3	Al_2O_3
SC-N0-HP	HP (1850 °C/1 h)	91	0	6	3
SC-N5-HP	HP (1850 °C/1 h)	86.5	5	5.7	2.8
SC-N10-HP	HP (1850 °C/1 h)	81.9	10	5.4	2.7
SC-N0-1650	HP (1850 °C/1 h)+AN (1650 °C/5 h)	91	0	6	3
SC-N5-1650	HP (1850 °C/1 h)+AN (1650 °C/5 h)	86.5	5	5.7	2.8
SC-N10-1650	HP (1850 °C/1 h) +AN (1650 °C/5 h)	81.9	10	5.4	2.7
SC-N0-1850	HP (1850 °C/1 h)+AN (1850 °C/5 h)	91	0	6	3
SC-N5-1850	HP (1850 °C/1 h) +AN (1850 °C/5 h)	86.5	5	5.7	2.8
SC-N10-1850	HP (1850 °C/1 h)+AN (1850 °C/5 h)	81.9	10	5.4	2.7

the higher eutectic temperature of the grain boundary phases, $RE_2Si_2O_7$ (RE=Er, Lu, Sc) compared to oxynitride phases.

Oxidation behaviour of SiC ceramics depends on many factors such as partial pressure of oxygen, temperature, grain boundary phase composition or amount of sintering additives. Silicon-based ceramics exhibit two types of oxidation behaviour, passive and active oxidation. During passive oxidation (according to Eq. (1)), mainly at low temperature and high oxygen partial pressure, a silica protective layer (SiO_2 film) is formed at the surface of SiC preventing in from further oxidation:

$$2SiC + 3O_2 \rightarrow 2SiO_2 + 2CO\uparrow \quad (1)$$

Active oxidation occurs at high temperature and low oxygen partial pressure, and no protective film is created because formation of vapour SiO (Eq. (2)):

$$SiC + O_2 \rightarrow SiO\uparrow + CO\uparrow \quad (2)$$

The oxidation behaviour of the SiC ceramics, fabricated by different routes, with many combination of sintering additives has been extensively investigated [21–28] but the oxidation resistance of SiC/Si_3N_4 composites with applied heat treatment after sintering has not been described yet. Suzuki et al. [21] significantly improved an oxidation resistance of LPS-SiC using high purity SiC powder with a minimal addition of Al_2O_3. Liu [22] observed that the oxidation (temperatures in interval of 1200–1350 °C, exposure time of 60–120 h) of pressureless liquid-phase-sintered (PLPS) SiC with Y_2O_3–Al_2O_3 sintering additive content is in all case passive with formation of protective oxide scales, and that the oxidation resistance decreases with increasing additive content. Rodríguez-Rojas et al. [23] confirmed passive and protective oxidation and the decrease of oxidation resistance with increasing sintering additive content (oxidising temperature of 1500 °C, exposure time of 500 h). At these temperatures the oxidation kinetics of PLPS SiC had two stretches. The first was described by the arcan-rate law and the second by the parabolic-rate law. The partial

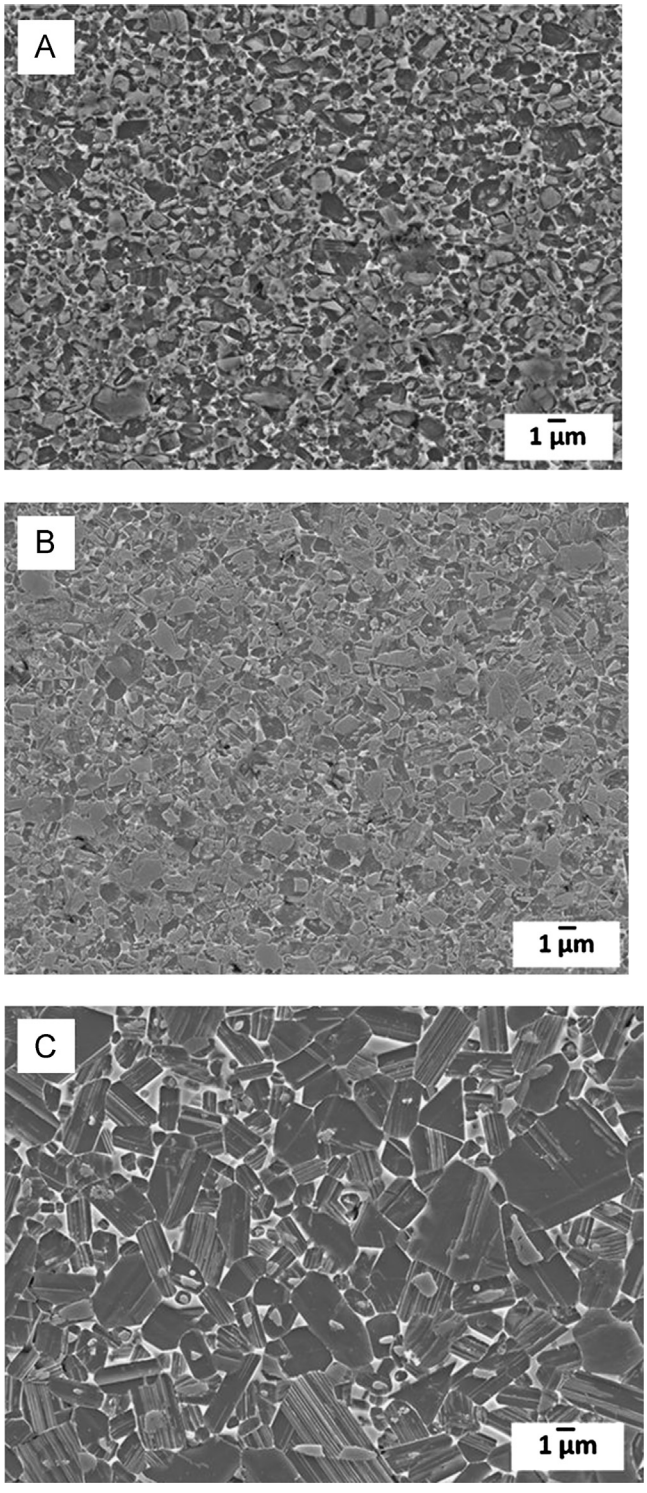

Fig. 1. SEM micrographs of (a) SC-N5-HP; (b) SC-N5-1650; (c) SC-N10-1850.

crystallisation of the oxide scales during the first hours of the oxidation is responsible for this complex oxidation kinetics. Biswas et al. [24] investigated SiC–Lu_2O_3–AlN system. The material showed high oxidation resistance at and below 1400 °C however the oxidation resistance degraded significantly at 1500 °C. Mangani et al. [25] prepared SiC–AlN–RE_2O_3 (RE = Y, Yb, Er, Lu, Ho, Sm, Ce) composites. These composites

Table 2
Properties of SiC and SiC/Si_3N_4 composites.

Samples	ρ (g/cm^3)	HV5 (GPa)	K_{IC} (MPa m$^{1/2}$)	ΔW (mg/cm^2)	k_p (kg^2/m^4 s)
SC-N0-HP	3.220	20.4 ± 0.9	3.19 ± 0.2	2.31	7.26 × 10−10
SC-N5-HP	3.236	19.7 ± 0.6	3.27 ± 0.1	2.11	6.08 × 10−10
SC-N10-HP	3.249	20.6 ± 0.7	3.55 ± 0.1	2.63	9.40 × 10−10
SC-N0-1650	3.220	19.4 ± 1.3	3.62 ± 0.5	2.43	8.03 × 10−10
SC-N5-1650	3.224	20.4 ± 0.7	3.89 ± 0.1	1.69	3.91 × 10−10
SC-N10-1650	3.241	20.8 ± 1.1	4.32 ± 0.3	2.75	1.03 × 10−9
SC-N0-1850	3.189	20.6 ± 0.3	4.68 ± 0.3	0.32	1.39 × 10−11
SC-N5-1850	3.196	22.5 ± 0.8	5.15 ± 0.5	0.15	3.12 × 10−12
SC-N10-1850	3.204	20.7 ± 1.1	4.86 ± 0.3	0.29	1.15 × 10−11

showed a high oxidation resistance at 1500 °C. Oxidation followed a parabolic rate law with migration of RE^{3+} ions as rate-limiting step. Choi et al. [26] fabricated SiC–AlN–RE_2O_3 (RE = Y, Er, Yb) by hot pressing and subsequent annealing. SiC with AlN and rare-earth oxides showed superior oxidation resistance compared with SiC–YAG and SiC–Al_2O_3–Y_2O_3–CaO.

The aim of this study is to investigate the influence of heat treatment on hardness, fracture toughness and oxidation resistance of liquid-phase-sintered SiC–Si_3N_4 composites.

2. Experimental materials and methods

2.1. Starting material and experimental setup

β-SiC powder (HSC-059, Superior Graphite) was mixed with Al_2O_3 (A 16 SG, Alcoa), Y_2O_3 (grade C, H.C. Starck) and Si_3N_4 (AlY-3/54, Grade C, Plasma & Ceramic Technologies Ltd.). The Si_3N_4 powder contains Y_2O_3 and Al_2O_3 sintering additives in weight ratio 6:3. The weight ratio of nonoxide matrix to oxide sintering additives SiC (+Si_3N_4):Y_2O_3+Al_2O_3 was kept constant, 91:9. The weight ratio of particular oxides Y_2O_3:Al_2O_3 was 6:3 for all compositions. The final chemical compositions of the investigated materials are listed in Table 1.

The powder mixtures were ball milled in isopropanol with SiC balls for 24 h. The suspension was dried and subsequently sieved through 25 μm sieve screen in order to avoid hard agglomerates. The samples were sintered by hot pressing at 1850 °C/1 h under mechanical pressure of 30 MPa in N_2 atmosphere. The hot pressed samples were subsequently annealed under various temperature conditions given in Table 1. After sintering and annealing the specimens were cut, polished to a 1 μm finish and etched in Murakami solution. The microstructures were then studied using an SEM (JEOL JSM-7000F) and X-ray diffraction (CuKα radiation, Philips, Eindhoven, the Netherlands).

2.2. Density, hardness, fracture toughness and oxidation resistance

The densities of the sintered and annealed specimens were measured according to Archimedes' principle in water.

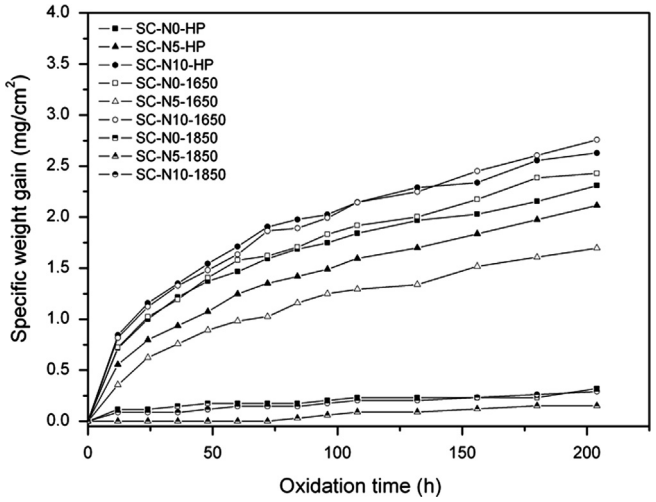

Fig. 2. Specific weight gain as a function of oxidation time (T = 1350 °C).

Hardness was determined by Vickers indentation (hardness testers LECO 700AT) under a load of 49.05 N for 10 s and calculated by the following equation:

$$HV = \frac{1.8544\ x\ P}{d^2}\ (Mpa) \tag{3}$$

HV—Vickers hardness, P—indentation load, d—average diagonals length of indent.

The fracture toughness was determined by the Single Edge V-Notched Beam method [29]. In the case of a 4-point flexure with spans of 40 and 20 mm, the fracture toughness is then calculated by the following equations:

$$K_{IC,SENVB} = \sigma\sqrt{aY} = \frac{F}{B\sqrt{W}} \cdot \frac{S_1 - S_2}{W} \cdot \frac{3\sqrt{\alpha}}{2(1-\alpha)^{1,5}} \cdot Y \tag{4}$$

$$Y = 1.9887 - 1.326\alpha - \frac{\left(3.49 - 0.68\alpha + 1.35\alpha^2\right)\alpha(1-\alpha)}{(1+\alpha)^2} \tag{5}$$

$$\alpha = \frac{a}{W} \tag{6}$$

K_{IC}—fracture toughness, σ—fracture strength, F—fracture load, B—specimen thickness, W—specimen width, S_1—outer span distance, S_2—inner span distance, a—average V-notch length, α—relative V-notch depth, Y—stress intensity shape factor.

The specimens with dimensions 3 × 4 × 25 mm were used for oxidation tests. Before testing they were diamond polished to a 1 μm finish. After grinding and polishing to reduce roughness, the specimens were cleaned in an ultrasonic bath and degreased with acetone and ethanol. Dried samples were then weighed and the exact dimensions were measured in order to calculate the surface area. The oxidation experiments were performed in a furnace at 1350 °C in air, for time in the range 0–204 h. At intervals, the bars were removed from the furnace, weighed to compute the specific mass change (Δm), and returned for further oxidation. After oxidation tests the surface of oxidised samples was observed by SEM with EDS analysis.

3. Results and discussion

3.1. Microstructure

All ceramic samples were well densified. The relative density increases from 97.2% to 99.1% with silicon nitride addition from 5 to 10 wt%. The density was slightly decreased by increasing the annealing temperature.

Representative microstructures of a polished and chemically etched surface of the SiC/Si_3N_4 composites are shown in Fig. 1. The microstructures of hot pressed SC-N5-HP (Fig. 1a) and SC-N5-1650 composite annealed at 1650 °C (Fig. 1b) consist of fine submicron-sized equiaxed SiC grains with a low aspect ratio (~1). No visible effect of the heat-treatment at 1650 °C was found on the microstructure of the material. In the case of SiC–Si_3N_4 composite the addition of silicon nitride resulted in a finer microstructure of the composites [30]. Phase analysis of the hot pressed and annealed materials at 1650 °C showed β-SiC as a major phase. All the materials additionally contain secondary phase content of crystalline YAG. The microstructures of the SiC material and SiC–Si_3N_4 composites significantly changed after their post-sintering high temperature treatment at 1850 °C (Fig. 1c). They have a bimodal distribution and consist of elongated SiC grains with higher aspect ratio (3.5–4.4) and of smaller SiC and Si_3N_4 grains. All the annealed materials contained α-SiC as a major phase indicating the occurrence of β→α phase transformation, and secondary phase content of crystalline YAG.

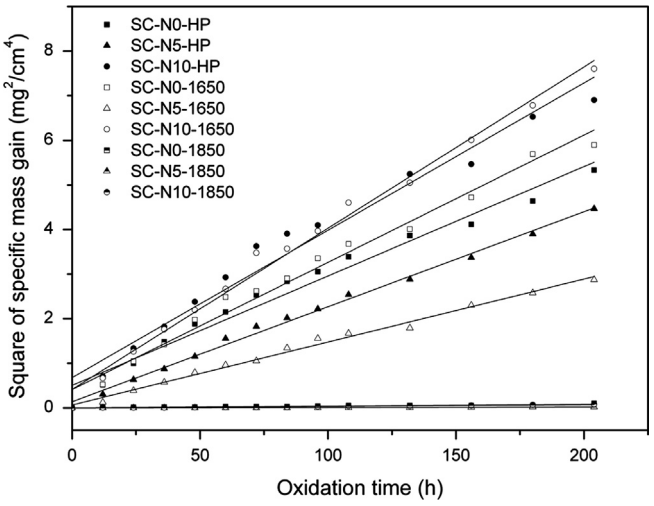

Fig. 3. Square of the specific weight gain as a function of the oxidation time (T=1350 °C).

3.2. Hardness and fracture toughness

The results of the hardness and fracture toughness measurements are shown in Table 2. During heat treatment, the average grain size (G) increased in all systems and hence invoking Hall-Petch like H vs. $G^{1/2}$ behaviour, hence one would expect a decrease in hardness (H) values with increasing average grain size [31]. However, in poly-crystalline ceramics containing glassy grain boundary and intergranular phases, after thermal treatment, reduction and crystallisation of the secondary phases generally improve the hardness of the material [7]. In our case no significant change in the values of hardness (in the range from 19.5 to 22.5 MPa) due to the heat treatment and silicon nitride addition has been observed.

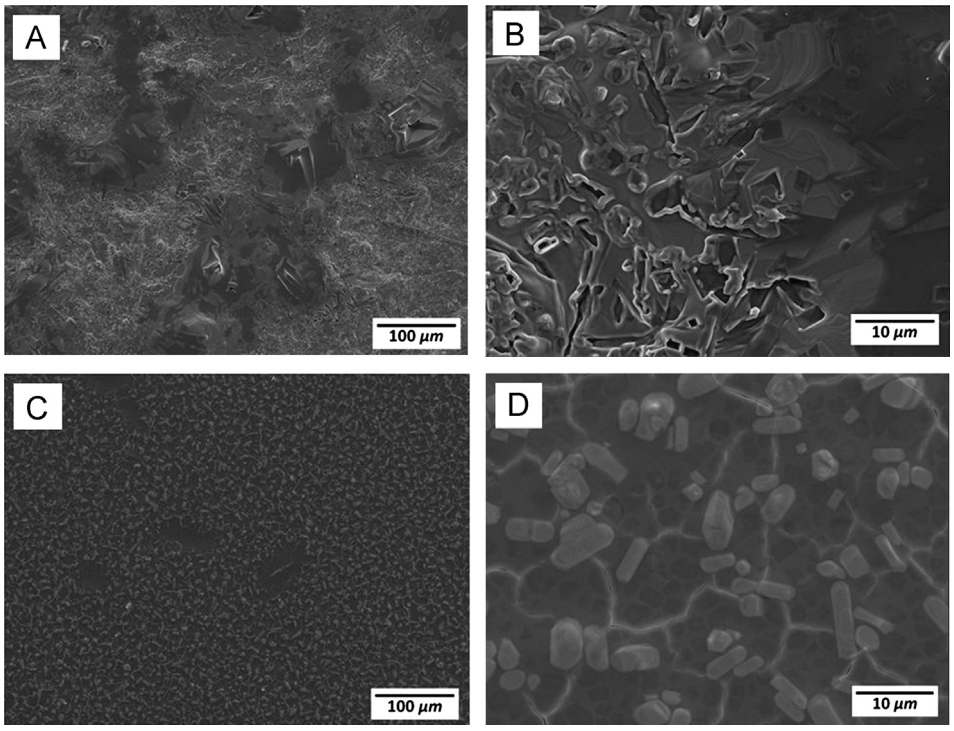

Fig. 4. SEM micrographs of oxidised surfaces of specimens (a) and (b) SC-N5-1650; (c) and (d) SC-N5-1850 after 204 h at 1350 °C in air.

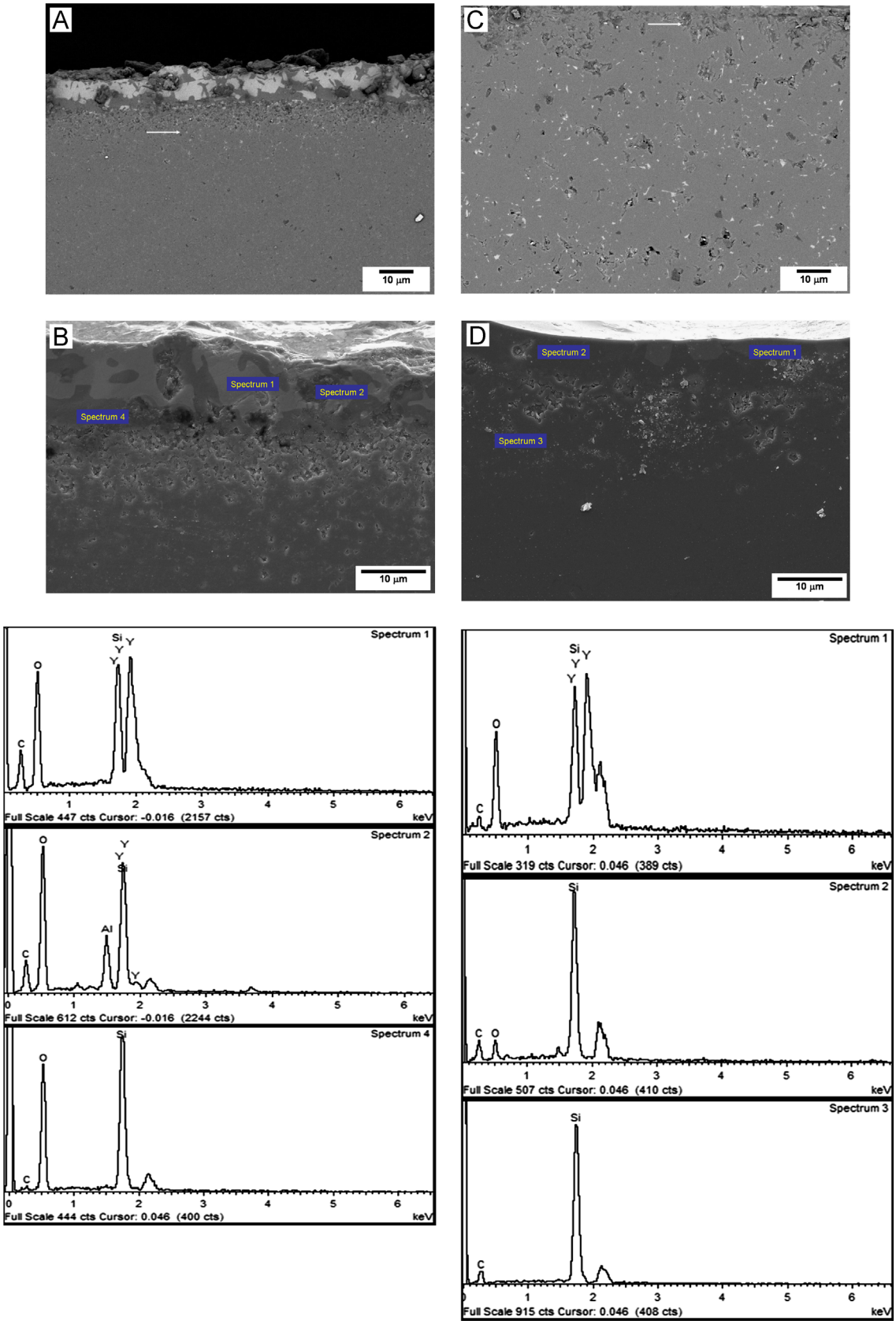

Fig. 5. Cross-sections of the oxidised samples (a) SC-N10-HP; (b) SC-N5-1650 with EDS composition analysis; (c) SC-N5-1850; (d) SC-N10-1850 with EDS composition analysis after 204 h at 1350 °C in air.

According to the results, the fracture toughness is increased with annealing temperature. For fine-grained globular microstructure of hot pressed SiC and SiC–Si_3N_4 composites the fracture toughness had a value of K_{IC} in interval from 3.19 ± 0.2 to 3.55 ± 0.1 MPa $m^{1/2}$. After heat treatment at 1650 °C the fracture toughness increased and its values changed from 3.62 ± 0.5 to 4.32 ± 0.3 MPa $m^{1/2}$. For annealed materials at 1850 °C/5 h with plate-like microstructure the highest fracture toughness was obtained (from 4.68 ± 0.3 to 5.15 ± 0.5 MPa $m^{1/2}$). The relatively significant improvement of $K_{IC,\ ind}$ upon annealing at 1850 °C/5 h can be directly correlated with the larger grain size and higher aspect ratio despite some indication of transcrystalline fracture behaviour. Different mechanisms of toughening have been observed in these materials with plate-like microstructures [30].

3.3. Oxidation resistance

Fig. 2 is a plot of weight gain per unit surface area as a function of time at 1350 °C. All prepared SiC–Si_3N_4 composites and SiC monolithic ceramics show high oxidation resistance at 1350 °C. The materials with fine globular microstructure had a specific weight gains on the order of 1.7–2.7 mg/cm^2 after 204 h. Specimens with plate-like microstructure showed lower mass gain in the range of 0.15–0.29 mg/cm^2. Square of the specific weight gain as a function of oxidation time is shown in Fig. 3. According to the following equation, the slope of the straight lines corresponds to parabolic oxidation rate constants:

$$\Delta W^2 = k_p.t + Q \quad (7)$$

where ΔW^2 is the weight gain per unit surface area, k_p is the rate constant of parabolic oxidation, t is the exposure time and Q is an additive constant (ideally = 0).

Table 2 reports the parabolic oxidation rate constants for all experimental samples, as well as the total specific weight gains after 204 h. As can be seen there exist appreciable differences between the oxidation kinetics of material sintered, heat treated at 1650 °C and heat treated at 1850 °C. The specific mass gain and rate constant of parabolic oxidation decrease with increasing of annealing temperature. The sample SC-N5-1850 with the highest oxidation resistance in this study had a specific rate constant of 3.12×10^{-12} $kg^2\ m^{-4}\ s^{-1}$ at 1350 °C. This parabolic oxidation rate is about two orders of magnitudes lower compared to composite SC-N5-1650, $k = 3.91 \times 10^{-10}$ $kg^2\ m^{-4}\ s^{-1}$. This is good agreement with other authors [16,21]. Nevertheless, there is always mass gain throughout the oxidation period indicating that oxidation is passive because active oxidation is accompanied by mass loss.

The morphologies of the surfaces oxidised at 1350 °C at higher and lower magnifications are shown in Fig. 4. Surface of materials sintered and annealed at 1650 °C has inhomogeneous distributed oxidation products of different type and shape (Fig. 4a). The surface of materials annealed at 1850 °C was completely covered with smaller globular grains (Fig. 4c). The cross-sections of the oxidised layers can be seen in Fig. 5. The oxide layer thickness was determined to be approximately 15 μm for materials sintered and annealed at 1650 °C (Fig. 5a) and around 5 μm for materials annealed at 1850 °C (Fig. 5c). A few of pores were observed at the interface between the oxidised layer and SiC bulk, probably due to possible reactions between SiC and SiO_2, resulting in the formation of CO or CO_2 [33]. Analysis of the composition of the oxide layer by SEM/EDS revealed that the dark phase is predominantly composed of Si and O indicating the presence of SiO_2 while the brightest phase is composed of Y, Si and O indicating the presence of $Y_2Si_2O_7$ (Fig. 5d). Materials sintered and annealed at 1650 °C Al was also analysed indicating probably various aluminium silicates or yttrium aluminium silicates (Fig. 5b). SiC would react first with O_2 to form SiO_2 and CO. Then, part of the SiO_2 would react with YAG ($Y_3Al_5O_{12}$) to form $Al_2Si_2O_7$ and $Y_2Si_2O_7$. The formation of these silicates result in a zone depleted of Y^{3+} and Al^{3+} cations immediately bellows the oxide scale [32]. Guo et al. [11] reported the presence of $Er_2Si_2O_7$ phase either in the equaixed or in plate-like morphologies, dependent on oxidation temperature. It has been proposed that the parabolic oxidation behaviour indicates that the rate-limiting step is a diffusive process, either by oxygen diffusing trough a growing silica layer or by RE^{3+} (Y^{3+}) cations diffusing trough the oxide layer in the opposite direction [20,24,32].

4. Conclusion

The influence of the heat treatment on basic mechanical properties and oxidation behaviour of LPS SiC and SiC–Si_3N_4 was investigated. The following conclusion can be drawn:

The heat treatment especially at highest temperature of 1850 °C/5 h changed the microstructure significantly (the coarsening of the microstructure of experimental materials were observed because $\beta \rightarrow \alpha$ phase transformation of SiC take place) and leads to the fracture toughness increase. The influence of the heat treatment on Vickers hardness values was not observed.

The oxidation of LPS SiC and SiC–Si_3N_4 composites is always passive and protective. The kinetic follows the parabolic law indicated diffusion as the rate limiting mechanisms. The heat treatment at higher temperature has a positive effect on oxidation behaviour. In particular, SiC–Si_3N_4 composite with 5 wt% silicon nitride addition annealed at 1850 °C/5 h exhibits the lowest values of specific weight gain after oxidation at 1350 °C for 204 h.

It was found that the silicon nitride addition to SiC matrix has no influence in the improvement of oxidation resistance. However, more experiments at higher oxidation temperatures (1450–1500 °C) and longer oxidation period (500 h) are necessary for better understanding the oxidation mechanisms of prepared SiC–Si_3N_4 composites.

Acknowledgements

This work was partly supported by the Slovak Government through Projects APVV-0161-11, APVV 0500-10 and LPP-0203-07, and by the Centre of Excellence of Slovak Academy of Sciences CFNT-MVEP.

References

[1] L.K.L. Falk, Microstructural development during liquid phase sintering of silicon carbide ceramics, Journal of the European Ceramic Society 17 (1997) 983–994.

[2] A. Malinge, A. Coupé, S. Jouannigot, Y. Le Petitcorps, R. Pailler, P. Weisbecker, Pressureless sintered silicon carbide tailored with aluminium nitride sintering agent, Journal of the European Ceramic Society 32 (2012) 4419–4426.

[3] M. Nader, F. Aldinger, M.J. Hoffmann, Influence of the α/β-SiC phase transformation on microstructural development and mechanical properties of liquid phase sintered silicon carbide, Journal of Materials Science 34 (1999) 1197–1204.

[4] G.-D. Zhan, R.-J. Xie, M. Mitomo, Y.-W. Kim, Effect of β-to-α phase transformation on the microstructural development and mechanical properties of fine-grained silicon carbide ceramics, Journal of the American Ceramic Society 84 (2001) 945–950.

[5] N.P. Padture, In situ-toughened silicon carbide, Journal of the American Ceramic Society 77 (1994) 519–523.

[6] D.H Cho, Y.-W. Kim, W. Kim, Strength and fracture toughness of in situ-toughened silicon carbide, Journal of Materials Science 32 (1997) 4777–4782.

[7] D. Sciti, S. Guicciardi, A. Bellosi, Effect of annealing treatments on microstructure and mechanical properties of liquid-phase-sintered silicon carbide, Journal of the European Ceramic Society 21 (2001) 621–632.

[8] Y.-W. Kim, M. Mitomo, H. Emoto, J.-G. Lee, Effect of initial α-phase content on microstructure and mechanical properties of sintered silicon carbide, Journal of the American Ceramic Society 81 (1998) 3136–3140.

[9] Y.-W. Kim, M. Mitomo, H. Hirotsuru, Grain growth and fracture toughness of fine-grained silicon carbide ceramics, Journal of the American Ceramic Society 78 (1995) 3145–3148.

[10] J.J. Cao, W.J. Moberly Chan, L.C. De Jonghe, C.J. Gilbert, R.O. Ritchie, In situ toughened silicon carbide with Al–B–C additions, Journal of the American Ceramic Society 79 (1996) 461–469.

[11] S. Guo, N. Hirosaki, H. Tanaka, Y. Yamamoto, T. Nishimura, Oxidation behavior of liquid-phase sintered SiC with AlN and Er_2O_3 additives between 1200 °C and 1400 °C, Journal of the European Ceramic Society 23 (2003) 2023–2029.

[12] N.P. Padture, B.R Lawn, Toughness properties of a silicon carbide with an in situ induced heterogeneous grain structure, Journal of the American Ceramic Society 75 (1994) 2518–2522.

[13] M.A. Mulla, V.D. Krstic, Pressureless sintering of β-SiC with Al_2O_3 additions, Journal of Materials Science 29 (1994) 934–938.

[14] J.K. Lee, H. Tanaka, H. Kim, Microstructural changes in liquid-phase-sintered α-silicon carbide, Materials Letters 29 (1996) 135–142.

[15] G. Magnani, L. Beaulardi, Properties of liquid phase presureless sintered SiC-based materials obtained without powder bed, Journal of the Australian Ceramic Society 41 (2005) 31–36.

[16] R.P. Jensen, W.E. Luecke, N.P. Padture, S.M. Wiederhorn, High-temperature properties of liquid-phase-sintered α-SiC, Materials Science and Engineering A 282 (2000) 109–114.

[17] M. Balog, K. Sedlackova, K. Zifcak, J. Janega, Liquid phase sintering of SiC with rare-earth oxides, Silikaty 49 (2005) 259–262.

[18] K. Biswas, G. Rixecker, F. Aldinger, Effect of rare-earth cation additions on the high temperature oxidation behaviour of LPS-SiC, Materials Science and Engineering A 374 (2004) 56–63.

[19] H.J. Choi, Y.W. Kim, M. Mitomo, T. Nishimura, J.H. Lee, D.Y. Kim, Intergranular glassy phase free SiC ceramics retains strength at 1500 °C, Scripta Materialia 50 (2004) 1023–1027.

[20] G. Magnani, F. Antolini, L. Beaulardi, E. Burresi, A. Coglitore, C. Mingazzini, Sintering, high temperature strength and oxidation resistance of liquid-phase-pressureless-sintered SiC-AlN ceramics with addition of rare-earth oxides, Journal of the European Ceramic Society 29 (2009) 2411–2417.

[21] K. Suzuki, N. Kageyama, T. Kanno, Improvement in the oxidation resistance of liquid-phase-sintered silicon carbide with aluminum oxide additions, Ceramics International 31 (2005) 879–882.

[22] D.-M. Liu, Oxidation of polycrystalline a-silicon carbide ceramic, Ceramics International 23 (1997) 425–436.

[23] F. Rodríguez-Rojas, A.L. Ortiz, O Borrero-López, F Guiberteau, Effect of the sintering additive content on the protective passive oxidation behaviour of presureless liquid-phase-sintered SiC, Journal of the European Ceramic Society 32 (2012) 3531–3536.

[24] K. Biswas, G. Rixecker, F. Aldinger, Improved high temperature properties of SiC-ceramics sintered with Lu_2O_3-containing additives, Journal of the European Ceramic Society 23 (2003) 1099–1104.

[25] G. Mangani, F. Antolini, L. Beaulardi, A. Brentari, E. Buressi,Oxidation, resistance of SiC-AlN ceramics coated by oxidation-assisted-pack cementation process, Journal of the European Ceramic Society 31 (2011) 369–376.

[26] H.-J. Choi, J.-G. Lee, Y.-W. Kim, Oxidation behavior of liquid-phase sintered silicon carbide with aluminum nitride and rare-earth oxides, Journal of the American Ceramic Society 85 (2002) 2281–2286.

[27] K.A. Weidenmann, G. Rixecker, F. Aldinger, Liquid phase sintered silicon carbide (LPS-SiC) ceramics having remarkably high oxidation resistance in wet air, Journal of the European Ceramic Society 26 (2006) 2453–2457.

[28] B.G. Simba, C. Santos, M.J. Bondioli, K. Strecker, E.S. Lima, M. H. Prado da Silva, Strength improvement of LPS-SiC ceramics by oxidation treatment, International Journal of Refractory Metals and Hard Materials 28 (2010) 484–488.

[29] Advanced Technical Ceramics-Monolithic ceramics-Fracture toughness-Part 5: Single-edge V-notch beam (SENVB) method. European Standard. Third draft ENV 14425-5, April 2001.

[30] A. Kovalčíková, J. Dusza, P. Šajgalík, Thermal shock resistance and fracture toughness of liquid-phase-sintered SiC-based ceramics, Journal of the European Ceramic Society 29 (2009) 2387–2394.

[31] R.W. Rice, C.Cm. Wu, F. Borchelt, Hardness–grain-size relations in ceramics, Journal of the American Ceramic Society 77 (1994) 2539–2553.

[32] F. Rodríguez-Rojas, A.L. Ortiz, O. Borrero-López, F. Guiberteau, Effect of Ar and N_2 sintering atmosphere on the high-temperature oxidation behaviour of pressureless liquid-phase-sintered α-SiC in air, Journal of the European Ceramic Society 30 (2010) 119–128.

[33] M.J.F. Guinel, M.G. Norton, Blowing of silica microforms on silicon carbide, Journal of Non-Crystalline Solids 351 (2005) 251–257.